Annu. Rev. Fluid Mech. 2004. 36:149–72
doi: 10.1146/annurev.fluid.36.050802.121935

FLOW-RATE MEASUREMENT IN TWO-PHASE FLOW

Gary Oddie and J.R. Anthony Pearson
Schlumberger Cambridge Research, High Cross, Madingley Road, Cambridge CB3 0EL, United Kingdom; email: oddie@cambridge.oilfield.slb.com, pearson@cambridge.oilfield.slb.com

Key Words Venturi, gamma-ray, Coriolis, electromagnetic, flow meter

■ **Abstract** Online, continuous, two-phase flow measurement is often necessary, particularly in the oil and gas industry. In this article, we describe some of the commercially most important techniques for gas-liquid, gas-solid, liquid-solid, and liquid-liquid flows, and provide associated illustrative sketches and regime maps. These techniques involve Venturi pressure drop, Coriolis, electromagnetic, and cross-correlation flow meters, gamma-ray absorption and gradio-manometer densitometers, and local electrical and fiber-optic sensors, for which we describe the principles of operation and interpretation. References are given to more comprehensive texts and papers; these are representative rather than exhaustive. It is emphasized that empirical calibration is the norm and that detailed fluid-mechanical analysis has so far played little part in instrument design and operation.

1. INTRODUCTION

Choice of a meter (involving at least two separate measuring devices) to measure flow rates in two-phase flow (Hewitt 1978, Kremlevsky 2000) depends on the purpose for which the measurement is made, and the accuracy required. It also depends on the nature of the flow field and the two phases involved.

We cannot cover the subject exhaustively here, so we restrict detailed consideration to a few specific examples. In particular, we give most attention to pipe flows arising in industrial circumstances, where flow rates and geometries lead to unsteady and/or turbulent flow (see, for example, Baker 1954, Govier & Aziz 1972 for early references to the oil industry). The two extremes of vertical flow and horizontal flow are archetypal. By contrast, we do not attempt to discuss methods for mapping a two-phase velocity field at a small scale, except in the one instance of stratified horizontal flow. We see that most devices, though based on simple mechanical principles, rarely make use, for interpretation purposes, of a detailed mechanical understanding of the complex flow fields usually associated with the pipe flows involved. In many cases they rely largely on the results of empirical calibration.

It is a truism that (single-phase) flows of a homogeneous fluid are more accurately and reliably measurable than those of an inhomogeneous two-phase mixture (Baker 2000). Intimate mixing of the two phases is the simplest option for flow-rate measurement and most of the devices described below are based on single-phase flow meters that assume flat velocity profiles; separation into two single-phase streams is the next simplest option. (This latter is true even if the two phases are imperfectly separated before separate measurement of the two streams.)

We consider here the four distinct classes of two-phase flow: gas-liquid flow, gas-solid flow, liquid-solid flow, and liquid-liquid flow. For our purposes, solids are particulate, kinematically incompressible, and nondeformable; liquids are kinematically incompressible and continuously deformable; gases are both compressible and deformable. The large density ratio ρ_{solid}/ρ_{gas} (see Appendix) means that measurable gas-solid flows normally involve small particles and high speeds: We are not concerned with segregated flows as in wind-blown sands or moving fluidized beds. The similarly large density ratio ρ_{liq}/ρ_{gas} is less restricting in gas-liquid flows because of deformability and breakup of drops, and we discuss these in detail for both vertical and horizontal flows. Density ratios ρ_{solid}/ρ_{liq} and ρ_{liq1}/ρ_{liq2} can be far enough from unity in horizontal liquid-liquid and liquid-solid flows to lead to significant stratification, though in vertical flows the main effect is to lead to a relative slip velocity between the phases. When slip occurs, the mean fractional flow rates are different from their mean (instantaneous) fractions in the pipe.

When classifying devices used for metering, it is appropriate to consider time and length scales. The usual requirement for an industrial meter is for a global (integral over pipe cross-section) relatively long-time (an order of 1 minute) average flux for the two phases. Over longer time scales (of an order of 1 hour to 1 day) this time-average flow rate may change significantly. However, time scales associated with flow unsteadiness (typically of an order of 1 second or less for turbulent flow, but greater than 1 second for slug/plug flow in long pipes) are shorter than those over which time averages are taken. If we now consider the techniques used to make the flow measurements, these may be almost instantaneous (as in a pressure or pressure difference measurement, and hence capable of sensing turbulent fluctuations) or only meaningful over longer time scales (as in gamma-ray absorption measurements for mean density). The inverse frequencies of any sensing radiation can usually be taken to be very small times by comparison with kinematic fluctuation times. One may use either global or local (as when small devices are introduced into the flow field) techniques.

The global fluxes may be obtained either from a small number of global measurements or from integrals (more strictly weighted sums) over a large number of local flow (velocity and phase) measurements. The devices employed can be either nonintrusive (external to the flow field or, at most, part of the pipe/fluid interface) or intrusive (thus distorting the flow geometry at the place of measurement). Nonintrusive devices can use tomographic techniques to sense local characteristics of the motion. Some intrusive devices provide or assist (e.g., in the case of a static mixer) global measurements, and some (local optical, electrical, or pressure probes) provide local phase flow rates.

The relative magnitudes of the instrumental length scales (pipe diameter, probe tip radius, piezo-electric crystal diameter), the dispersed phase length scale (particle, drop or bubble "diameters," film thickness), and the wave length of the sensing radiation (whether electromagnetic or acoustic) restrict the nature of the information provided by any device and hence affect how fluxes are deduced.

It is almost always helpful to have overall kinematic information about phase distributions and phase velocities when selecting a measurement technique for a particular flow. In most cases experimental observations provide this. Fluid mechanical theories that predict or explain the observed kinematics (see e.g., Fabre & Line 1992, Crowe et al. 1996) play little part in the interpretation of measurements, although they can explain the form of observed correlations. The nomenclature of mixture theories (Drew & Passman 1999), interpreted as ensemble, spatial, or time averages, proves convenient and is adopted here when required.

2. GAS-LIQUID FLOW

2.1. Vertical Flow

This is a very well-investigated class of flows (advantage is often taken of the buoyancy of the gas phase to help drive an upward flow, as in oil well gas-lift). It is usual to define a series of flow regimes (Hewitt & Hall-Taylor 1970, Spedding & Nguyen 1980) and to provide regime maps with the mean superficial phase velocities q_{gas} and q_{liq} (or dimensionless parameters based on them) as coordinates. Figure 1 gives typical sketches of the nature of the main regimes: bubbly, plug (or slug), churn, annular, and droplet.

Figure 2 shows a typical regime map. The boundaries between the regimes are somewhat subjective; they depend on the pipe diameter D, the small parameter $N_\rho = \rho_{gas}/\rho_{liq}$, the density ρ_{liq}, the viscosity μ_{liq}, the interfacial tension σ, the contact angle χ (the measure of wettability), and the surface roughness; as q_{gas} and q_{liq} increase, the regime boundaries are given by these two parameters alone. The most important dynamical and kinematical variables describing the flow are the vertical mean pressure gradient $\partial P/\partial z$ and the mean gas fraction α_{gas} as functions of the imposed velocities q_{gas}, q_{liq}, and all the other constitutive parameters.

All relations can be made dimensionless with characteristic length D, velocity $(gD)^{1/2}$, and time $(D/g)^{1/2}$, and the dimensionless parameters N_ρ, $N_\mu = \mu_{gas}/\mu_{liq}$, χ, $N_{cap} = \mu_{liq}(gD)^{1/2}/\sigma$, $N_{grav} = \rho_{liq} gD/\mu_{liq}$, $N_L = L/D$. A large literature testifies to the difficulty of predicting $\partial P/\partial z$ and α_{gas} theoretically.

The demand for gas-liquid flow meters arises preeminently in the oil industry for monitoring production at the well head. (The measurement of steam-water flows in boiler pipes represents another important application.) We concentrate here on a Venturi-based meter (Atkinson et al. 1999, 2000, 2002) that is remarkably adaptable to a wide range of flow conditions. The objective is to predict, online

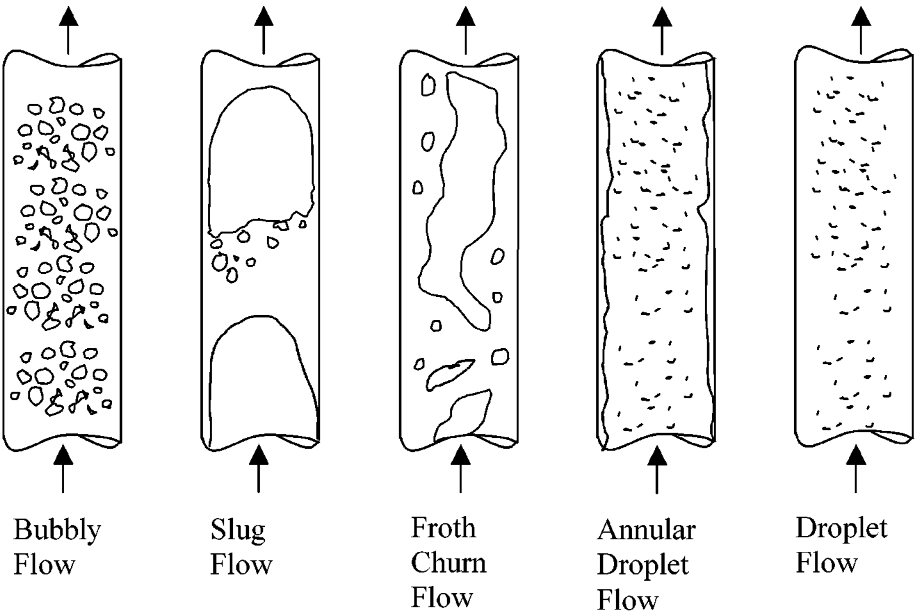

Figure 1 Sketches of vertical gas-liquid flow patterns (after Hewitt & Hall-Taylor 1970).

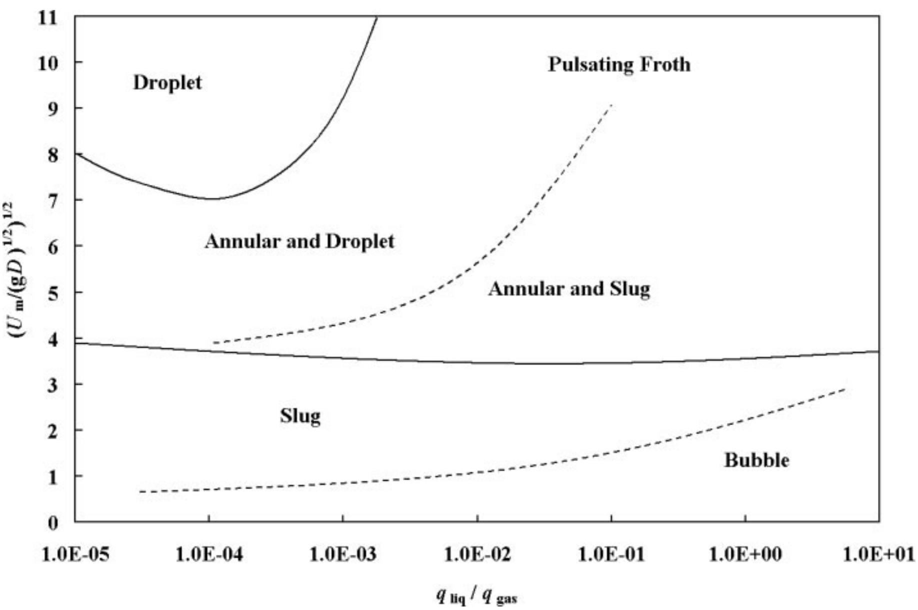

Figure 2 Typical vertical upwards gas-liquid flow regime map (after Spedding & Nguyen 1980).

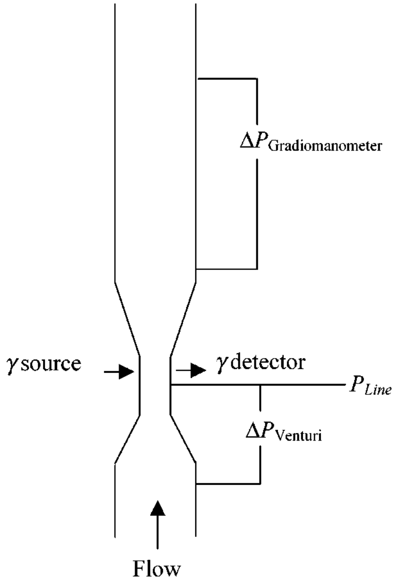

Figure 3 Sketch of Venturi (after Atkinson et al. 2000), showing position of γ-ray detector and gradio-manometer.

and continuously, the total mass flow rates M_{gas}, M_{liq} given direct measurements of ΔP and α_{gas}.

Figure 3 gives a simplified view of an axial (axi-symmetric) section of the flow channel of the Venturi. In the following discussion, we reference density measurements using the γ-ray densitometer. We discuss the gradio-manometer in Section 4. The pressure drop between entry and throat is interpreted to a first approximation using Bernouilli's equation for steady single-phase flow of a fluid of density ρ and mass flow rate M.

$$M = \frac{\pi D^2}{4}\left(\frac{2\rho\Delta P}{1-\beta^4}\right)^{1/2}, \quad \beta = \frac{D_{throat}}{D} \tag{1}$$

Even for incompressible single-phase flow, a small correction factor, the discharge coefficient, $C(\mathrm{Re}) \sim 0.99$ for large $\mathrm{Re} = 4M/\pi D\mu$, is added to the right-hand side of Equation 1 to account for pressure loss and wall boundary layers. A further correction factor ε can be included to account for fluid compressibility (see ISO 1991). These are shown in Equation 4.

If there is little or no slip between the phases ($\alpha_{gas} = \gamma_{gas}$) and the two phases are well dispersed and homogeneous, Equation 1 applies where

$$\rho_m = \alpha_{gas}\rho_{gas} + (1-\alpha_{gas})\rho_{liq} \tag{2}$$

and

$$M_{total} = M_{gas} + M_{liq} = \{\rho_{gas}\alpha_{gas} + \rho_{liq}(1 - \alpha_{gas})\} Q_{total} \tag{3}$$

replace ρ and M. Although μ in Re above is not well defined, the corrections C and ε are retained. If accuracy tolerates an error of say 5–10% throughout the likely dynamic range, then the averaged no-slip model gives an acceptable result, certainly for M_{total}.

Obviously large relative errors in M_{gas} and M_{liq} (Atkinson et al. 2002) arise when α_{gas} approaches 1 because the slip velocity is likely very important (e.g., in annular flow) and $s = u_{gas}/u_{liq}$ is significantly different from 1. An improved form for Equations 1 and 3 can be written (Atkinson et al. 2000) as

$$M_{total} = C(\mathrm{Re})\varepsilon \frac{\pi D^2}{4} \left(\frac{2\Delta P \rho_m}{1 - \beta^4} \right)^{1/2} \tag{4}$$

where

$$M_{gas} = \frac{M_{total}\alpha_{gas}\rho_{gas}}{\alpha_{gas}\rho_{gas} + (1 - \alpha_{gas})\rho_{liq} s}. \tag{5}$$

Much attention has been paid to modeling high-gas flows (defined by the requirement that $M_{gas}/M_{liq} \geq \mathrm{O}(1)$ and thus relevant to gas wells), though the theories developed have been used largely to suggest suitable empirical functional forms for the relative slip, whose precise quantitative form is obtained by experiment (De Leeuw 1997, Steven 2001). The effects of liquid-gas phase transitions also affect the interpretation (Elperin et al. 2002).

The great advantage of the Venturi mass flow rate meter is that it provides a direct global measurement and is not directly intrusive in the sense of penetrating into the flow. It also has no moving parts and can be made into a robust instrument. The accelerations achieved into the throat are local only in the sense that there is a near-uniform axial variation in cross-section. This is true even for bull-nosed entrance inlets to the throat.

Above it is assumed that α_{gas} is known. γ-ray absorption, which is proportional to the total mass traversed for suitably chosen γ-ray energies and carefully collimated beams, is now the preferred means for measuring ρ_m, whence $(1 - \alpha_{gas})$ follows directly, assuming ρ_{liq} is known and N_ρ is negligibly small. The collimated beam's path is not exactly representative of the cross-section in that it is weighted towards small values of the radial coordinate r. This can be significant in the case of liquid wall layers, though the Venturi "conditions" the flow in or just upstream of the throat, probably by stripping off wall layers.

In practice, the gas and liquid (mostly methane and crude oil at thermodynamic equilibrium in our simple example) densities are functions of temperature and pressure, so both have to be measured at the meter. To get the necessary pressure/volume/temperature (PVT) relations for any particular crude oil, one must take a sample of the flowing fluid, on which off-line measurements are made.

For slug and churn flows, there are large variations in α_{gas} on time scales of an order of $\rho_m D^3/M_{total}$, i.e., for times comparable with the time of mean mass flow through the Venturi. Although variations in ΔP can be followed accurately in time by the differential pressure device, reliable values for α_{gas} can only be obtained by the γ-ray device in the throat as relatively long-time averages. The precise way in which the necessary averages for $\rho^{1/2}$ and $\Delta P^{1/2}$ are obtained, bearing in mind the inherent instrumental errors for the two devices, affects the accuracy of the overall value obtained for M_{total} (see Atkinson et al. 1999, 2000, 2002 for details). Figure 4*a*,*b* indicates the accuracies achieved by commercially available instruments.

Some commercial meters use nonintrusive microwave devices to measure ρ_m indirectly (Nyfors 2001). Theory suggests that the electromagnetic response of the flowing fluid depends significantly on the geometrical distribution of the phases, i.e., on the details of the regime involved. Not surprisingly, interpretations of measurements are wholly empirical and specific to the device; their advantage is a very fast response time. Also, a pair of such devices mounted one upstream of the other can provide time-of-flight and hence mean velocity estimates. The relevant time-of-flight is obtained from the delay between the (two) time series from the pair of devices that maximizes their cross-correlation coefficient. Dynamic range and accuracy tend to be limited and there is uncertainty in what velocity is measured. Electromagnetic flow meters were also applied to these flows (Baker & Deacon 1983, Cha et al. 2001).

In most producing oil wells, water is coproduced with crude oil as a result of a high connate water saturation in the reservoir or water breakthrough during a water drive from injector wells. Thus, there is a phase consisting of two liquids. The water-to-liquid ratio (WLR) is often an even more important quantity to measure than the gas-to-oil ratio (GOR). Measuring the WLR as well as the M_{total} and the GOR demands a three-phase meter. The Venturi/γ-ray combination described above can be altered to do this by using twin γ-ray beams of different energies, whose absorption/scattering behavior depends nonlinearly on the atomic weight of the material in the path of the beam. There is negligible slip between water and oil when interpreting M_{liq} as $M_{oil} + M_{water}$. Alternatively, one can attempt partial online separation, whereby a representative liquid stream can be obtained, thus allowing a well-tested range of devices to measure the WLR.

2.2. Horizontal Flow

Although the Froude number $N_{Fr} = gD/u_m^2$ is formally the same for vertical and horizontal flow, orthogonality between the mean velocity and gravity vectors means that axi-symmetry will be lost in horizontal flow and mean density stratification will ensue. This suggests that global measurements will not suffice unless there is a deliberate attempt to mix the phases (e.g., using a static mixer) before measurement (e.g., with a Venturi/γ-ray two-phase meter). Figures 5 and 6 show relevant regimes and a regime map. In general, there is little need to meter two-phase horizontal

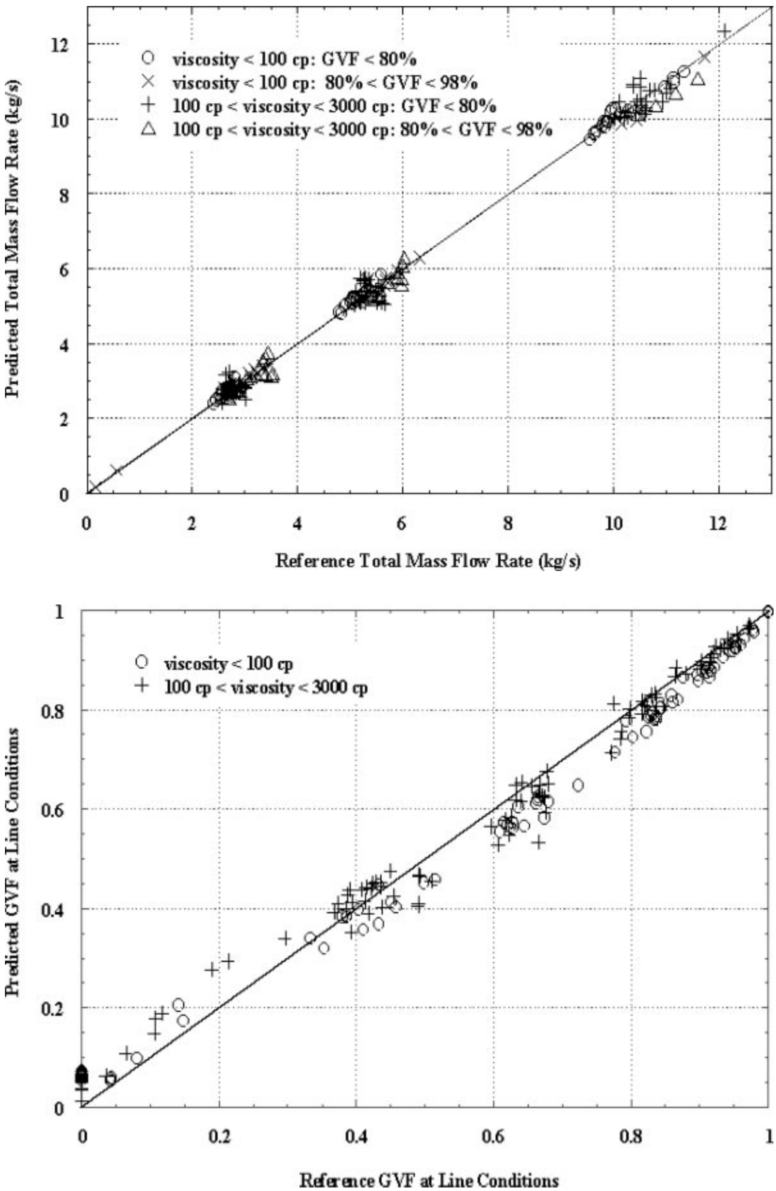

Figure 4 Venturi X™ data plots (*a*) M_{total}, (*b*) GVF (after Atkinson et al. 2000).

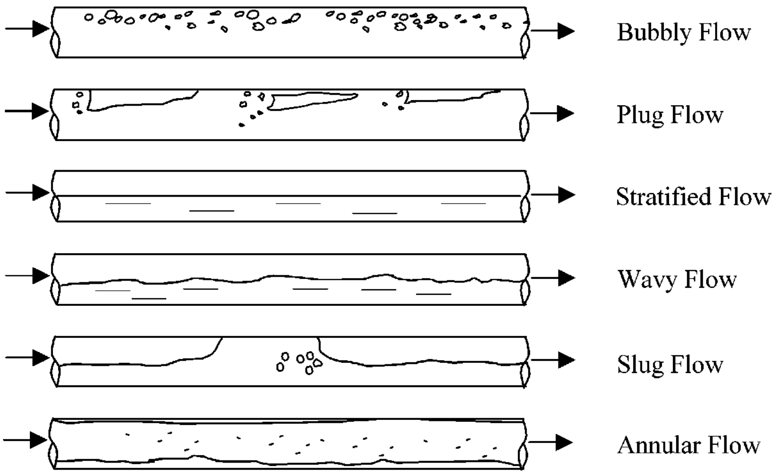

Figure 5 Sketches of horizontal gas-liquid flow patterns (after Hewitt & Hall-Taylor 1970).

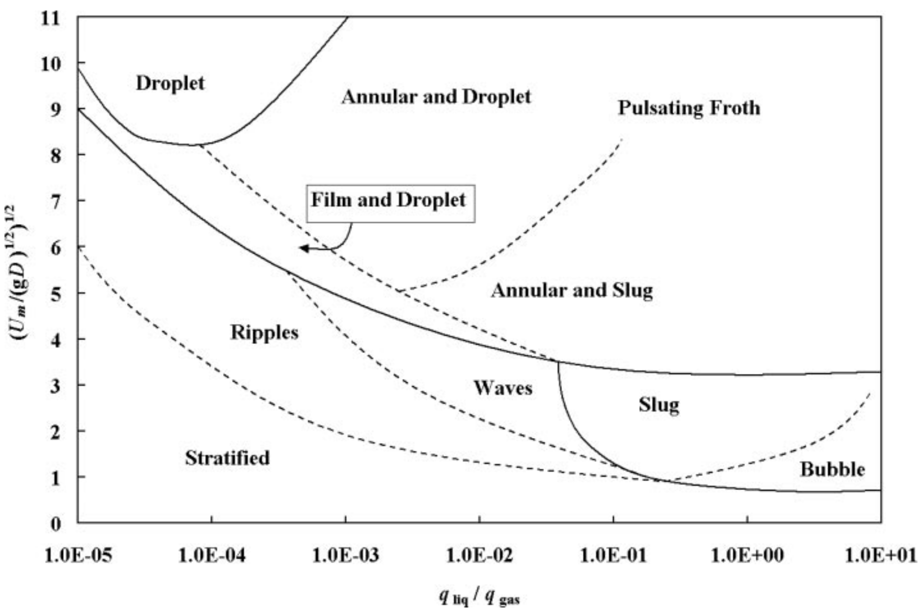

Figure 6 Typical horizontal gas-liquid flow regime map (after Spedding & Nguyen 1980).

flows, given that metering is easier in the vertical orientation: In most industrial situations pipe-work is designed to follow a sequence of horizontal and vertical paths; one of the latter can be chosen. An exception arises in the case of horizontal oil wells, where there is a need to monitor the production rates along the well. In most cases the gas is a minor component so we discuss measuring techniques in detail in Section 4.2.

2.3. Inclined Flow

No major departures in behavior arise from what is described for the extreme (vertical and horizontal) cases. For flows inclined at no more than $\pi/4$ rad to the vertical, techniques for the vertical case can be used. However, regime boundaries are most sensitive to inclination for values close to the horizontal, and so in practice when the angle of inclination along a "horizontal" pipe varies slightly (as is the case for horizontal wells), unsteady and complex phase distributions arise (even during steady production conditions) (Oddie et al. 2003) (see Figure 13).

3. SOLID-GAS AND SOLID-LIQUID FLOW

We consider these two classes of two-phase flow in pipes together here largely because online flow measurement of both phases is impractical except in fully-suspended and essentially homogeneous flow. For solid-gas flow, this implies fine particles or powders in rapid gas flow. Two-phase measurement techniques developed for equivalent concentrations of liquid drops in a fast gas stream are generally suitable. (There are many commercially important examples of pneumatic transport of solid particles, such as seed grains, polymer granules, or crushed minerals where the gas phase is air; stratification, settling, and saltation will likely occur. However, any metering required will then be for the solid phase alone, which is most easily carried out when the particles are at rest in containers.)

For solid-liquid flow, suspension is more easily achieved because of smaller density ratios and higher continuous phase viscosity. At one extreme are fine slurries that can be treated as single-phase fluids; the base fluid viscosity can be low whereas the effective single-phase viscosity (often shear-rate dependent) rises rapidly with solid fraction; in many cases the flow is laminar and any required metering involves specialized devices and techniques (Baker 2000, Miller 1996). At the other extreme are relatively dilute (mean) concentrations of rapidly sedimenting particles in turbulent water flow (leading to bed formation and transport at the bottom of horizontal or near-horizontal pipes). Figures 7 and 8 give typical regime maps from which a user can assess when particular measurement devices might be suitable. We now describe two interesting techniques, successful for single-phase pipe flow measurement, that can be adapted to provide solid-liquid and liquid-liquid (and, in the case of the electromagnetic flow meter, gas-liquid) flow measurements.

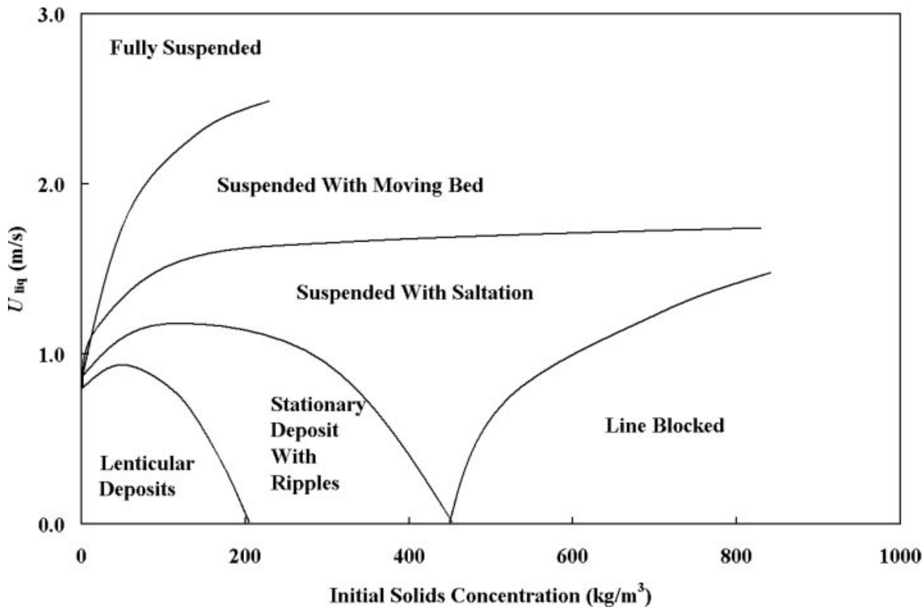

Figure 7 Horizontal flow of mono-disperse (60 μm) glass beads in 20-mm diameter pipe (after Newitt et al. 1955).

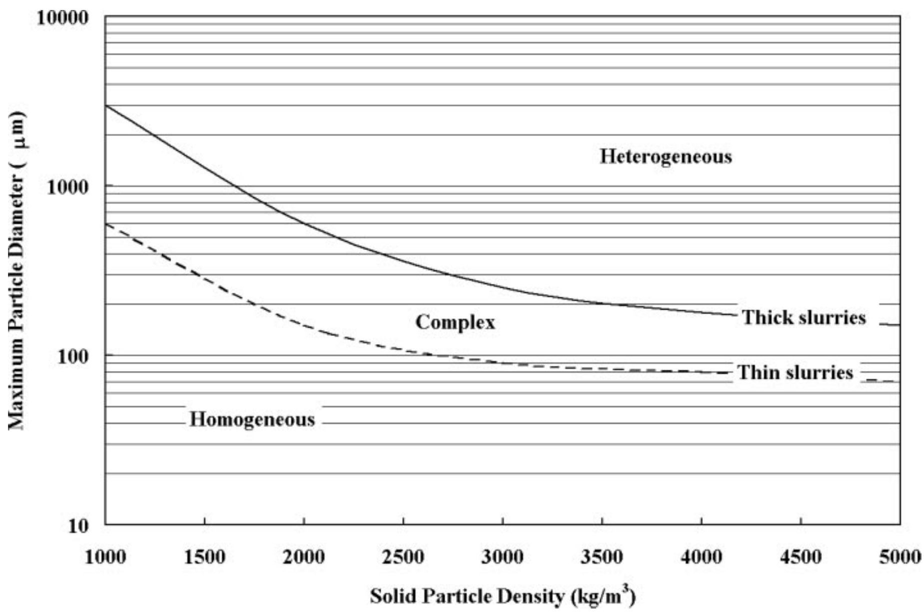

Figure 8 Flow regimes for water-based slurry flows, in a horizontal pipe at 1–2 m/s (after Cheremisinoff 1985).

3.1. Coriolis Flow Meter

The physical principle on which it is based is the Coriolis force, given locally by $\mathbf{F} = \rho\mathbf{u} \times \boldsymbol{\omega}$, where $\mathbf{u}$ is the fluid velocity and $\boldsymbol{\omega}$ the fluid vorticity. Figure 9 illustrates its most elementary application to pipe flow: the inlet pipe with its L-BEND and short exit section rotate at fixed angular velocity ω. Assuming a uniform fluid speed u in the rotating pipe arm of length R, the torque on the pipe will be $^1/_2 M\omega a^2$, where $M = {}^1/_4\pi\rho u D^2$ is the mass flow rate. Figure 10*a* shows a flow meter employing the principle directly (Li & Lee 1953), though its mechanical complexity and intrusive nature make it somewhat impractical.

Modern Coriolis meters are nonintrusive and involve small electrically imposed periodic displacements of chosen sections of the flow pipe. The frequency of the imposed displacement is varied over a finite range so as to achieve resonance. This resonant frequency and its Q, the quality factor of a resonant system, depends on many factors specific to any particular design. Suffice it to say that one can determine directly the density of the fluid filling the pipe (Young 1990) from the effect of its mass on the resonant frequency, and that the imposed displacement is chosen to lead to a small periodic vorticity in the flow, orthogonal to the pipe axis, which is in quadrature ($\pi/2$ out of phase) with the displacement. Thus, the periodic vorticity acts to dampen the oscillation. A full mechanical analysis of the system is nontrivial and geometry specific. The effect is very weak so successful quantitative detection depends on sensitive sensors and finely tuned electrical circuitry. Figure 10*b*,*c*,*d* shows three variants (Baker 1994, 2000).

Implicit in all interpretations of the actual measurements is that the flow remains uniform across the pipe and, in solid-liquid or liquid-liquid mixtures, that the phases do not slip relative to one another when oscillated and are not compressible. This makes the meter unsuitable for solid-gas or gas-liquid flows (Grumski & Bajura 1984). The great advantage of Coriolis meters is that they can make two measurements, of density and mass flow rate, respectively, and can be viewed as true two-phase meters. Cheesewright et al. (2000), Dimaczek et al. (1994), and

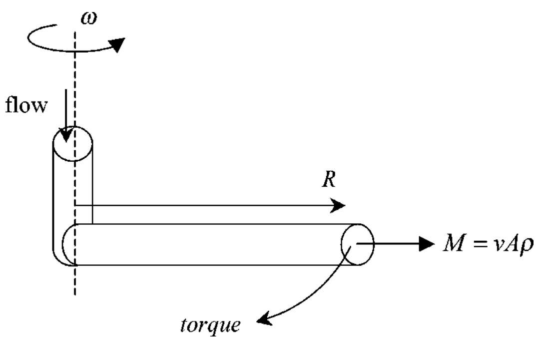

Figure 9 Sketch of the Coriolis principle.

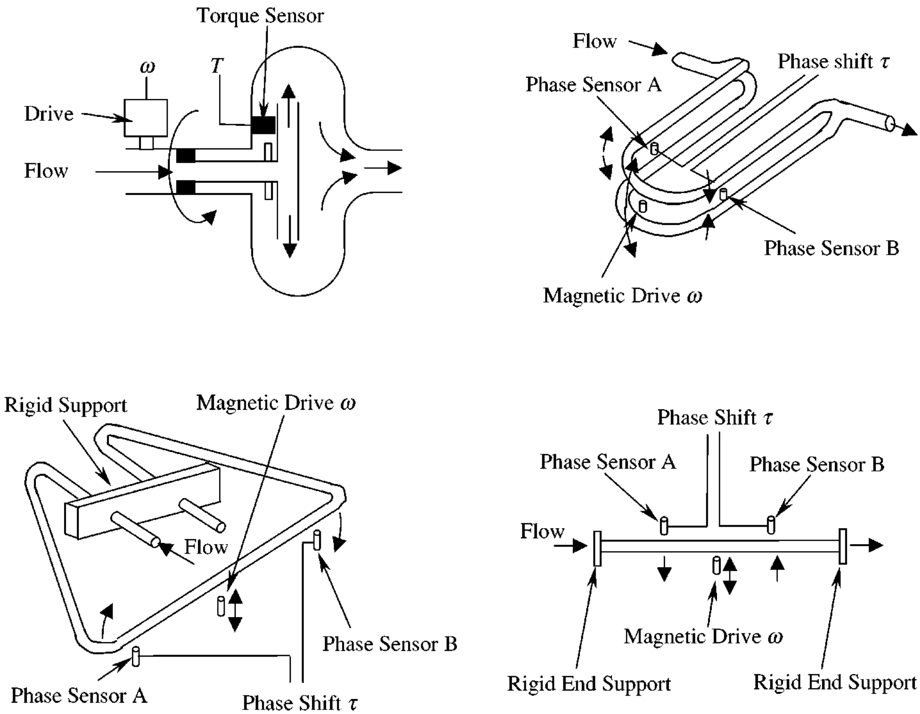

Figure 10 Classes of Coriolis mass flow meter. (*a*) Rotating element, (*b*) twin tube, (*c*) convoluted single tube, and (*d*) straight tube.

Dominick et al. (1987) provide details of particular instruments and calibration techniques.

3.2. Electromagnetic Flow Meter

A material moving with velocity **u** in a magnetic field **B** experiences an electromotive force $\mathbf{E}^* = \mathbf{u} \times \mathbf{B}$. If a low-frequency magnetic field **B** normal to the axis of flow in a pipe is imposed, then an electric potential field will be induced in the third (orthogonal) direction, also normal to the pipe. The basic principle of the electromagnetic flow meter is that this field can be sensed and measured, and that it is proportional to the flow velocity (Baker 2000, Shercliff 1962).

The simplest way to do this (see Figure 11) is to use an insulating pipe for the flow meter section and to sense the electric field through two electrodes positioned diametrically opposite one another in the insulated pipe and in contact with the continuous liquid phase, assumed conductive (Durcan 1998 discusses limits on conductivity). In general, a small current, driven by the induced electric field, is measured and interpreted to yield **u**, at least in single-phase flow. The actual electric field producing the current will be of the form $\mathbf{E} + \mathbf{u} \times \mathbf{B}$, where **E** will not

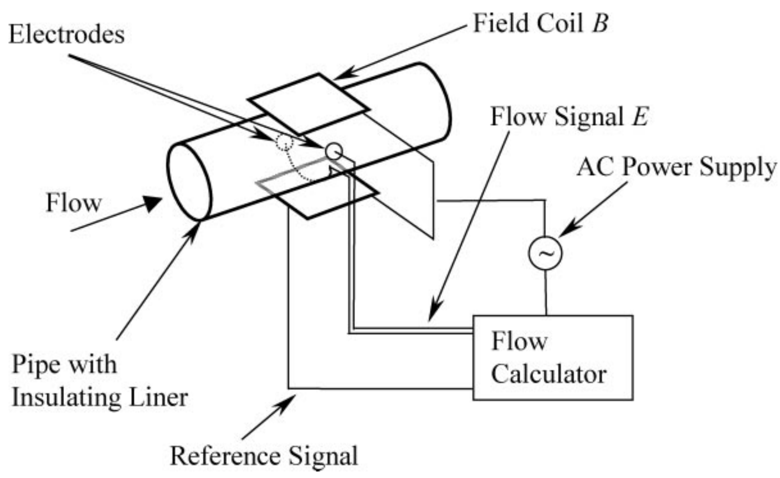

Figure 11 Basic electromagnetic flow meter.

be uniform and adjusts itself to satisfy the boundary conditions at pipe walls and electrodes, and the requirement that the current $\mathbf{j} = r(\mathbf{E} + \mathbf{u} \times \mathbf{B})$ be solenoidal, where r is the resistivity.

Interpretation in the case of two-phase fluid flow depends on the electrical conductivities and magnetic susceptibilities of the continuous and dispersed phases, as well as their velocities and geometrical distribution; the wetting characteristics of the electrodes can also be crucial. The details are nontrivial (Shercliff 1962, Krafft 1993, Wyatt 1986, Bevir 1970; for gas-liquid flow applications see Cha et al. 2001, Murakami et al. 1990; for solid-liquid applications see Heywood et al. 1993, Heywood & Mehta 1999) and are not examined here. Calibration is required; these devices work best in highly turbulent flows. An advantage of electromagnetic (EM) meters is that they are nonintrusive and have no moving parts, but in general separate measurement of density or phase holdup is required; a disadvantage is their reliance on the electrical conductivity of the continuous phase.

4. LIQUID-LIQUID FLOW

4.1. Vertical Flow

Because the ratio $N_\rho = \rho_{liq1}/\rho_{liq2}$, with $liq1$ the denser liquid, usually lies between 1 and 1.5, any flow for which the Froude number $N_{Fr} = (\rho_{liq1} - \rho_{liq2})gD/\rho_{liq1}u_m^2$ is $\leq$O(1) likely has one liquid well dispersed as drops within the other and the slip $1 - s$ will be $\ll$1 where $D_{drop}/D \ll 1$. The Venturi device introduced in the gas-liquid section is therefore likely suitable for direct mass flow rate measurement.

For laminar flow in a pipe, the viscous pressure gradient is given by

$$\left(\frac{dP}{dz}\right)_{visc} = -\frac{32 u_m \mu_{eff}}{D^2}, \tag{6}$$

where μ_{eff} lies between 1 and up to 100 times the viscosity of the continuous liquid. The hydrostatic pressure gradient is

$$\left(\frac{dP}{dz}\right)_{hyd} = \rho_m g. \tag{7}$$

The ratio of these gradients is given by

$$N_P = \frac{\rho_m g D^2}{32 u_m \mu_{eff}} = {}^1\!/_{32} N_{Fr} N_{\mathrm{Re}}. \tag{8}$$

For turbulent flow, Equation 6 is replaced by

$$\left(\frac{dP}{dz}\right)_{visc} = -f_m(\mathrm{Re}) \frac{\rho_m u_m^2}{2D}, \tag{9}$$

where f_m is the mixture friction factor and Equation 8 becomes

$$N_P = \frac{2 N_{Fr}}{f_m(\mathrm{Re})}. \tag{10}$$

For Re $> 10^4$, f_m is O(3×10^{-2}), therefore from Equation 10 $N_P \sim 70\ N_{Fr}$. For Re $= 10^3$, $N_P \sim 30\ N_{Fr}$ from Equation 8. Thus, if N_{Fr} is O(1), N_P is large and the density ρ_m can be obtained to an accuracy of $(N_P)^{-1}$ by using the pipe as a gradio-manometer (see also Fordham et al. 1999b). Therefore, the alternative geometry shown in Figure 3 is relevant for a gradio-Venturi meter with the pressure gradient in the pipe being measured above or below the throat. The liquid fraction α_{liq1} is obtained from the simple relation

$$\alpha_{liq1}\rho_{liq2} + (1 - \alpha_{liq1})\rho_{liq2} = \rho_m. \tag{11}$$

Obviously, the Venturi provides M_{total} from Equation 1 and hence u_m, μ_m, from which estimates for $(dP/dz)_{visc}$ can be obtained using Equation 7 or 9. Iteration using the gradio equation

$$\Delta P_{grad} = l_{grad}\left\{\left(\frac{dP}{dz}\right)_{visc} + \left(\frac{dP}{dz}\right)_{hyd}\right\} \tag{12}$$

gives significantly more accurate results, particularly if experiments provide empirical relations for μ_m and f_m(Re).

An alternative, intrusive, device based on local probes has metered vertical or near-vertical flows. The basic principle behind the device is that the leading tip of each probe, which points directly upstream, does not disturb the oncoming flow of dispersed drops sufficiently to alter the instantaneous presence function (for either phase) at the probe tip—this is equivalent to saying that the probe does not disturb (is "invisible" to) the flow at its tip, even though the total device is highly intrusive and inevitably alters the flow field downstream of the probe tip. The probe tip must be able to detect which phase (oil or water) surrounds it; it must also be able to discriminate between phases in a time short compared with that for a drop to pass and must sense a volume very small compared with the volume of a drop. In practice, neither this requirement of strictly local measurement volumes nor the invisibility of the probe to the flow are achieved, and much effort was spent in studying the "burbulent" (an unsteadiness associated as much with the buoyant rise of liquid drops as with mean high-Reynolds-number tube flow) passage of drops past a probe (Ramos et al. 2001, Pearson 2001). The physical techniques used are electrical (low-frequency impedance measurement) or optical (reflectance measurement at the interface between the end of a glass fiber or crystal tip and surrounding liquid).

The direct measurements described above yield a local value of α_{liq1}, which can either be taken as representative of the global value wherever it is measured in the cross-section, or can be measured at different positions in the cross-section for use in an integrating procedure. A further means is needed to measure the flow rates of the phases. One ingenious approach is to make the above "drop passage" measurements at different known "logging" speeds, i.e., by moving the probe at different speeds relative to the fixed pipe axially along it. This will yield different time series for the arrival of drops at the probe and different distributions for their time of passage, from which an estimate for the mean drop speed can be obtained.

A single drop of diameter d_{drop} moving vertically upwards at speed u_{drop} will pass a stationary probe in a time d_{drop}/u_{drop}, and one moving downwards at speed U_{probe} in a time $d_{drop}/(u_{drop} + U_{probe})$. If the ratio of these times is known, and this should be independent of drop size, then u_{drop}/U_{probe} can be calculated directly. The value of u_{drop} follows if U_{probe} is known. In a real flow, one must make assumptions about the stationary (in time and space) nature of the statistics for the time series being sensed. These have been tested empirically (Fordham et al. 1999a) to derive error estimates.

A practical advantage (in oilfield applications) of using a logging tool is that it provides its own electrical power down its cable, whereas a fixed gradio-Venturi tool located near the bottom of a well has to be supplied with power either by battery or by a permanent hard wire from the surface. Optical and electrical probes can also discriminate between gas and liquid (Fordham et al. 1999d), and thus a three-phase flow can be metered (Fordham et al. 1999c).

4.2. Horizontal and Near-Horizontal Flow

The regime map for a strictly horizontal liquid-liquid pipe flow (see Figure 12) is not as elaborate as that for a gas-liquid flow (at least not for the flow rates considered here, which refer to down-hole sections of horizontal oil wells, where the gas volume fraction (GVF) is far less than at the surface and the volumetric flow

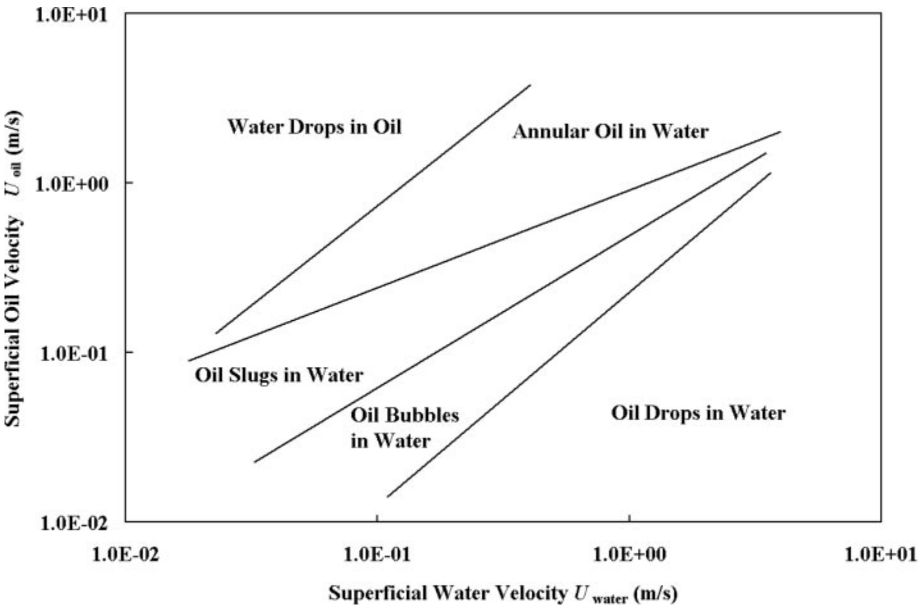

Figure 12 Horizontal oil-water flow regime map (after Charles et al. 1961).

rates are smaller). Because local phase velocities are smaller than those relevant in gas-liquid flow, a considerable degree of stratification arises, often leading to three principal strata: a lower, almost single-phase water, layer; a middle two-phase oil-in-water layer; and an upper, almost single-phase oil, layer. However these layers are not well defined; the upper or lower layers may be absent, and the instantaneous "interfaces" between the layers may be wavy and unsteady. The superficial velocities within each layer will differ from one another, particularly when the pipe is slightly inclined to the horizontal, even though the flows can be fully turbulent in all layers. Figure 13*a*,*b* provides sketches of phase distributions and a typical regime map for oil-water flow in wells at all inclinations.

Elaborate production-logging tools (see Figure 14) were developed to meter these two-phase (and in many cases when the bottom-hole pressure has fallen below the oil bubble point three-phase) flows over several hundreds of meters of well. The flow rates increase from toe to heel because oil and/or water are produced all along the horizontal section; the orientation of the well axis fluctuates along its length both because of imperfect "steering" during the drilling operation and because the producing layer may not be flat; in some cases (e.g., in uphill flow) reverse flow may arise in the lower layer and water may sometimes be caught in local sumps, usually leading to periodic fluctuations in local holdups (see Figure 15 for an illustrative sketch). Therefore, it is necessary to use a multiprobe device that spans the cross-section, thus sampling the flow in each layer simultaneously. As explained above, the general principles on which interpretation for phase holdups

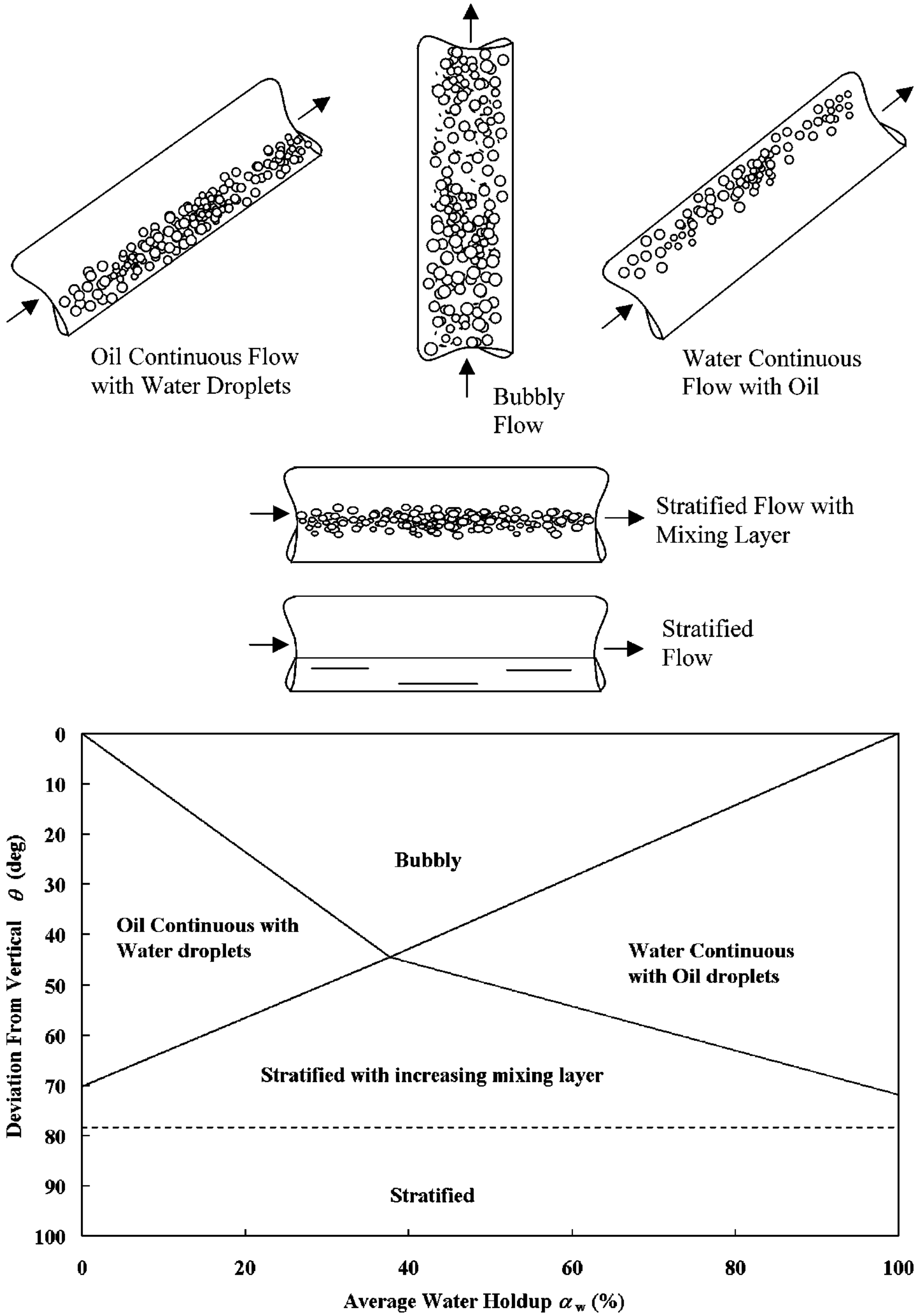

Figure 13 Down-hole oil-water flow: effect of inclination (*a*) sketches and (*b*) regime map.

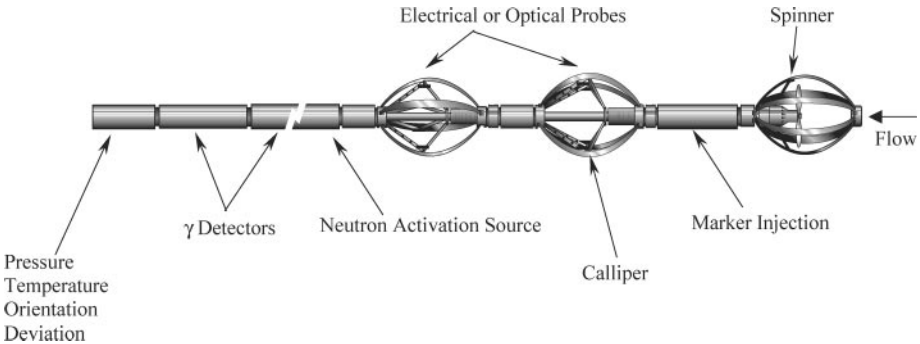

Figure 14 Flagship™ production logging tool and components.

α_{oil}, α_{water} is based still hold (cross plots are common; though it is not practicable to derive phase-velocities by logging at different speeds).

This flow meter incorporates several distinct measurements that are combined and interpreted to give estimates of the fractions and velocities of each phase (Theron 1993). Beginning with a well established turbine meter (spinner), which works well for high velocity and slipless flows, other techniques employed

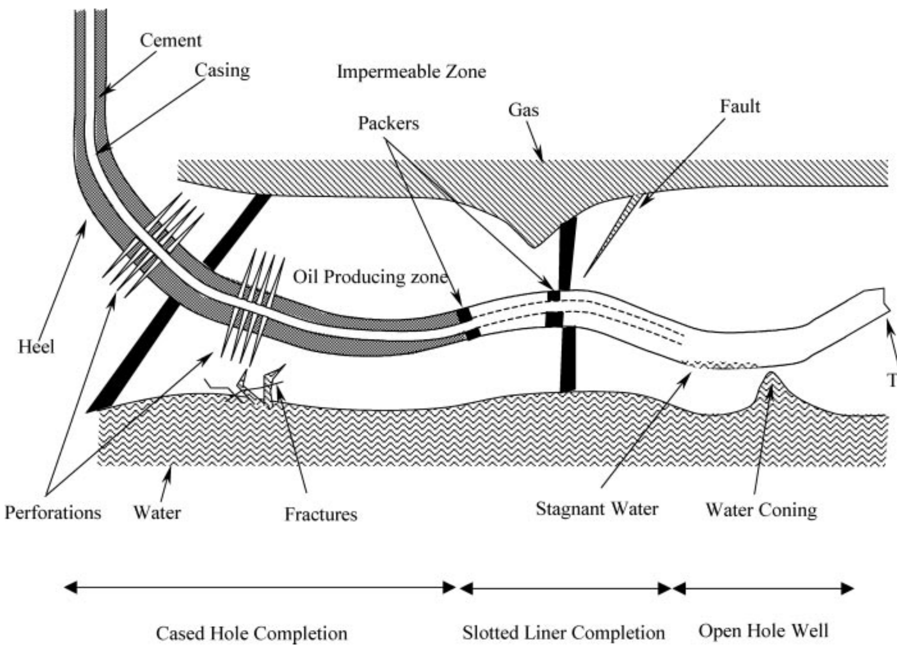

Figure 15 The down-hole environment.

include time-of-flight measurements on injected radio-nuclide tracers (Roscoe et al. 1996), where a neutron source activates a phase-specific marker and the resulting γ-ray decay is detected at two points further along the tool, giving a single-phase velocity via cross-correlation (Beck & Plaskowski 1987). Local probes (electrical or optical) then detect the relative proportions of the phases and can also be cross-correlated to give local and larger scale single-phase velocities. Combined with pressure, temperature, deviation (and orientation), and caliper measurements (especially in open-hole geometries), these velocities allow volumetric flow rate estimates to be made for each of the phases along the length of the producing zone.

Further global measurements are also available, such as cross-correlated electrical impedance measurements when one phase is continuous, carrying a second phase in discontinuous waves. For local holdup measurements, dielectric-sensitive probes can also be used, and in pairs, they can be cross-correlated to give local axial velocity.

Development continues on new and more accurate and robust measurement and interpretation techniques, but on the whole the approaches only take into account the effects of gross fluid distributions and empirical calibrations for the devices. There is still much room for an improved understanding of the interaction of phase and velocity distributions on these and all other flow measurement technologies.

Direct measurement of local velocity by small "spinners" (in the manner used globally in single-phase vertical well logging) has proven feasible, and cross-correlation of neutron activated tracer measurements and electrical impedance measurements, both made over axial lengths significantly greater than the well radius and thus expected to sample the full cross-section. Separate tracers can be dissolved in oil or water, so each mean velocity is obtained separately.

CONCLUSION

This article has presented only a brief overview of some techniques used for flow-rate measurement in two-phase flow. The actual measurements are not directly of the flow velocities and densities characteristic of the flow fields involved: They are almost always electrical voltages (or currents), which are related to physical quantities such as pressure, force, electrical potential, resonant frequency, spectral absorption or cross-correlation, caused or influenced by the flow field. These primary measurements or secondary (derived) flow-field variables have to be interpreted to yield the global flow rates. The accuracies demanded in flow metering are severe (of an order of 1% and rarely $>5\%$). Therefore, detailed simulations of two-phase flow, even using the best computational fluid dynamics (CFD) software available, can rarely predict phase distributions and velocities or pressures with sufficient accuracy for acceptable interpretation of secondary variables to be carried out on a theoretical a priori basis.

Success in two-phase flow measurement depends critically on empirical calibration (between the "measured" secondary variables dependent on the flow and the known imposed flow rates of each phase) for any chosen two-phase flow metering system. Commercial success also depends on the quality of the devices used to relate the primary measurements to the values of the (secondary) flow field variables being sensed, where accuracies of the order of $\ll 1\%$ are expected.

APPENDIX

$\mathbf{B}$	magnetic field
C	discharge coefficient
D, D_{throat}, d_{drop}	diameter (pipe, throat of Venturi, drop)
$\mathbf{E}$, $\mathbf{E}^*$	electric field
f_m	mixture friction factor
GVF	gas volume fraction
$\mathbf{j}$	current vector
l_{grad}	length of gradio-manometer
L	length of pipe
M, M_{gas}, M_{liq}, M_{total}, M_{oil}, M_{water}	mass flow rate (single-phase, gas, liquid, total, oil, water)

$N_{cap} = \mu_{liq}(gD)^{1/2}/\sigma$, $\quad N_{Fr} = gD/u_m^2$ or $(\rho_{liq1} - \rho_{liq2})gD/\rho_{liq1}u_m^2$,
$N_{grav} = \rho_{liq}gd/\mu_{liq}$, $\quad N_L = L/D$, $\quad N_P = (dP/dz)_{hyd}/(dP/dz)_{visc}$,
$N_\mu = \mu_{gas}/\mu_{liq}$, $\quad N_\rho = \rho_{gas}/\rho_{liq}$

P	mean pressure (function of z)
ΔP, ΔP_{grad}	mean pressure drop (Venturi, gradio-manometer)
q_{gas}, q_{liq}	superficial velocity (gas, liquid)
Q_{total}	total mean volume flow rate
r	electrical resistance
Re	Reynolds number
$\boldsymbol{s}$	$\boldsymbol{u_{gas}/u_{liq}}$ **or** $\boldsymbol{u_{liq2}/u_{liq1}}$
u_m, u_{gas}, u_{liq}, U_{probe}	speed (mean, gas, liquid, probe)
$\mathbf{u}$	fluid velocity
WLR	water to liquid ratio
z	axial coordinate
α_{gas}, α_{liq1}	mean phase volumetric fraction (holdup of gas, liquid1)
β	area contraction in Venturi throat
γ_{gas}	mean phase volumemetric flow rate fraction (gas)
χ	contact angle
ε	pressure coefficient
μ, μ_{liq}, μ_{eff}	viscosity (single-phase, liquid, effective)

ρ, ρ_m, ρ_{gas}, ρ_{liq}, ρ_{solid}	density (single-phase, mean, gas, liquid, solid)
ω	speed of rotation
$\boldsymbol{\omega}$	vorticity

ACKNOWLEDGMENT

We are grateful for Dr. D.I. Atkinson's help during the preparation of this article.

The *Annual Review of Fluid Mechanics* is online at http://fluid.annualreviews.org

LITERATURE CITED

Atkinson I, Berard M, Hanssen B-V, Ségéral G. 1999. New generation multiphase flowmeter from Schlumberger and Framo Engineering AS. *Proc. 17th Int. North Sea Flow Meas. Workshop, Oslo*. pp. 154–65

Atkinson DI, Berard M, Ségéral G. 2000. Qualification of a non-intrusive multiphase flow meter in viscous flows. *SPE Pap. 63118. Annu. Technical Conf. and Exhibition, Dallas, TX*

Atkinson DI, Pinguet B, Ségéral G, Theuveny BC. 2002. Field implications of uncertainties in multiphase flow measurements. *SPE Pap. 77403 Annu. Technical Conf. and Exhibition, San Antonio, TX*

Baker O. 1954. Simultaneous flow of oil and gas. *Oil Gas J.* 53:185

Baker RC. 1994. Coriolis flowmeters: industrial practice and published information. *Flow Meas. Instrum.* 5(4):229–46

Baker RC. 2000. *Flow Measurement Handbook. Industrial Designs, Operating Principles, Performance, and Applications,* Chapt. 17. Cambridge, UK: Cambridge Univ. Press, pp. 398–426

Baker RC, Deacon JE. 1983. Tests on turbine, vortex and electromagnetic flowmeters in two phase air-water upward flow. *Int. Conf. Phys. Model. Multi-phase Flow, Coventry, Engl., 19–21 April*, pp. 33–52

Beck MS, Plaskowski A. 1987. Cross correlation flowmeters: Their design and application. IOP

Bevir MK. 1970. Theory of induced voltage electromagnetic flow measurement. *J. Fluid Mech.* 43:577

Cha J-E, Ahn YC, Kim M-H. 2001. Flow measurement with an electromagnetic flowmeter in two-phase bubbly and slug flow regimes. *Flow Meas. Instrum.* 12(5–6):329–40

Charles ME, Govier CW, Hodgson GW. 1961. Horizontal pipeline flow of equal density oil-water mixtures. *Can. J. Chem. Eng.* 39(1):27–36

Cheesewright R, Clark C, Bisset D. 2000. The identification of external factors which influence the calibration of Coriolis massflow meter. *Flow Meas. Instrum.* 11(1):1–10

Cheremisinoff NP. 1985. *Encyclopedia of Fluid Mechanics,* Vol. 5: *Slurry Flow Tech*. Houston, TX: Gulf

Crowe CT, Trott TR, Chung JN. 1996. Numerical models for two-phase turbulent flows. *Annu. Rev. Fluid Mech.* 28:11–43

De Leeuw R. 1997. Liquid correction of Venturi meter readings in wet gas flow. *North Sea Flow Meas. Workshop, Kristiansand, Norway*

Dimaczek G, Fassbinder H-G, Emmel A, Kupfer R. 1994. High-precision coriolis mass flowmeter for bulk material two-phase flow. *Flow Meas. Instrum.* 5(4):295–302

Dominick J, Durst F, Raszillier H, Zeisel H. 1987. A method to measure mass and volume flow rates of two phase flows. *Int. J. Multiph. Flow* 13:685–98

Drew DA, Passman SL. 1999. *Theory of*

Multicomponent Fluids. New York: Springer-Verlag

Durcan LP. 1998. *Development of baseline stability in an electromagnetic flowmeter for dielectric liquids*. PhD thesis. Cranfield Univ., UK

Elperin T, Fominykh A, Klochko M. 2002. Performance of a Venturi meter in gas-liquid flow in the presence of dissolved gases. *Flow Meas. Instrum.* 13(1):13–16

Fabre J, Line A. 1992. Modelling of 2-phase slug flow. *Annu. Rev. Fluid Mech.* 24:21–40

Fordham EJ, Holmes A, Ramos RT, Simonian S, Huang S-M, Lenn CP. 1999a. Multiphase-fluid discrimination with local fibre-optical probes: I. Liquid/liquid flows. *Meas. Sci. Technol.* 10:1329–37

Fordham EJ, Lenn CP, Holmes A, Simonian S, Ramos RT. 1999b. Corrections of gradiomanometer data for volume fractions in two-phase flows. *Meas. Sci. Technol.* 10:N131–35

Fordham EJ, Ramos RT, Holmes A, Simonian S, Huang S-M, Lenn CP. 1999c. Multiphase-fluid discrimination with local fibre-optical probes: III. Three-phase flows. *Meas. Sci. Technol.* 10:1347–52

Fordham EJ, Simonian S, Ramos RT, Holmes A, Huang S-M, Lenn CP. 1999d. Multiphase-fluid discrimination with local fibre-optical probes: II Gas/liquid flows. *Meas. Sci. Technol.* 10:1338–46

Govier GW, Aziz K. 1972. *The Flow of Complex Mixtures in Pipes*. New York: Van Nostrand Reinhold

Grumski JT, Bajura RA. 1984. Performance of a Coriolis type mass flowmeter in the measurement of two-phase air-liquid mixtures. Mass flow measurements. *ASME Winter Annu. Meet., New Orleans*

Hewitt GF. 1978. *Measurement of two phase flow parameters*. London: Academic

Hewitt GF, Hall-Taylor NS. 1970. *Annular two-phase flow*. London: Pergamon

Heywood NI, Mehta KB. 1999. Performance evaluation of eight electromagnetic flowmeters with fine sand slurries. *Hydrotransport 14. BHRG*, pp. 413–31

Heywood NI, Mehta KB, Poplar D. 1993. Evaluation of seven commercially available electromagnetic flowmeters with Newtonian and non-Newtonian china clay slurry in pipeflow. *12th Int. Conf. Slurry Handling and Pipeline Transport–Hydrotransport 12. BHRG*, pp. 353–76

ISO 5167-1. 1991. Measurement of fluid flow by means of pressure differential devices

Krafft R. 1993. *Electromagnetic flowmeters in multiphase flows*. PhD thesis. Cranfield Inst. Technol., UK

Kremlevsky PP. 2000. Flow rate measurement in multiphase flows. Begell House

Li YT, Lee SY. 1953. A fast response true-mass-rate flowmeter. *Trans. ASME* l75:835–41

Miller RW. 1996. *Flow Measurement Engineering Handbook*. New York: McGraw-Hill

Murakami M, Maruo K, Yoshiki T. 1990. Development of an electromagnetic flowmeter for studying gas liquid two phase flow. *Int. Chem. Eng.* 30(4):699–702

Newitt DM, Richardson JF, Abbott M, Turtle RB. 1955. *Trans. Inst. Chem. Eng.* 33:93

Nyfors E. 2001. Permanent downhole microwave sensor for the local measurement of the water content of the fluid produced in an oilwell. *4th Int. Conf. Electromagnetic Wave Interaction with Water Moist Substances, Weimar, Ger*.

Oddie GM, Shi H, Durlofsky LJ, Aziz K, Pfeffer B, Holmes JA. 2003. Experimental study of two and three phase flows in large diameter inclined pipes. *Int. J. Multiph. Flow.* 29:527–58

Pearson JRA. 2001. The late stages of approach of liquid-liquid interfaces to smooth probes; rupture by asperities. *IUTAM Symp. Free Surface Flows, Birmingham, UK*, ed. AC King, YD Shikhmurzaev, p. 237. Dordrecht: Kluwer

Ramos RT, Holmes A, Wu X, Dussan E. 2001. A local optical probe using fluorescence and reflectance for measurement of volume fraction in multi-phase flows. *Meas. Sci. Technol.* 12:871–76

Roscoe BA, Lenn C, Jones TGJ, Whittaker

C. 1996. Measurement of the oil and water flow rates in a horizontal well using chemical markers and a Pulsed-Neutron Tool. *SPE Pap. 36563*, 6–9 Oct.

Shercliff JA. 1962. *The Theory of Electromagnetic Flow Measurement*. Cambridge, UK: Cambridge Univ. Press

Spedding PL, Nguyen PT. 1980. Regime maps for air water two phase flow. *Chem. Eng. Sci.* 35:779–93

Steven RN. 2001. Wet gas metering with a horizontally mounted Venturi meter. *Flow Meas. Instrum.* 12(5–6):361–72

Theron B. 1993. An integrated approach to production log interpretation. *SPE 8th Middle East Oil Show Conf., Bahrain, 3–6 April*

Wyatt DG. 1986. Electromagnetic flowmeter sensitivity with twophase flow. *Int. J. Multiph. Flow* 12(6):1009–17

Young A. 1990. Coriolis flowmeters for accurate measurement of liquid properties. *Adv. Instrum., ISA Proc.*, 45(4):1891–98

Annual Review of Fluid Mechanics
Volume 36, 2004

CONTENTS

INDEXES

ERRATA

An online log of corrections to *Annual Review of Fluid Mechanics* chapters may be found at http://fluid.annualreviews.org/errata.shtml